Materials Advances

ROYAL SOCIETY OF CHEMISTRY

PAPER

View Article Online
View Journal | View Issue

Cite this: *Mater. Adv.*, 2024, 5, 2400

Rapid detection of *Salmonella* using an aptamer-functionalized PDA liposome sensor with naked-eye colorimetric sensing†

Goeun Lee,[ab] Byeongsung Kim,[a] Inseung Jang,[a] Moon Il Kim,[c] Seunghan Shin[ad] and Kiok Kwon*[a]

The increasing occurrence of *Salmonella* pathogens responsible for foodborne diseases is of mounting global concern within the sphere of public health and consumer welfare. Detecting *Salmonella* holds pivotal importance in averting these illnesses. The complex pretreatment process, time-consuming nature, and expensive equipment associated with existing detection methods have posed barriers to the development of sensors capable of rapidly and effortlessly detecting pathogens in real-life scenarios. Therefore, the development of a colorimetric sensor capable of rapid and facile pathogen detection, without the need for complex sample preparation or expensive detection equipment, is a crucial research direction for ensuring food safety. In this study, we successfully engineered a PDA-based liposome sensor decorated with an aptamer that specifically interacts with *Salmonella typhimurium*, enabling the rapid and accurate detection of *Salmonella via* a colorimetric response. This aptamer-functionalized PDA sensor exhibited a distinct color change (colorimetric response of 15.7% for 1×10^4 CFU mL^{-1} *Salmonella*) within 15 minutes, accompanied by a highly linear increase in the CR values as the *Salmonella* concentration increased. In addition, the developed sensor materials can also effectively detect *Salmonella* in real food through a colorimetric reaction. We developed a colorimetric biosensor capable of detecting foodborne pathogens like *Salmonella*, with the naked eye in a simple and fast way, which demonstrates promising potential for sensor materials that could be extensively utilized in practical applications.

Received 11th October 2023,
Accepted 14th January 2024

DOI: 10.1039/d3ma00840a

rsc.li/materials-advances

1. Introduction

Foodborne illnesses caused by pathogenic microorganisms like *Salmonella*, *Listeria*, *Staphylococcus*, and *Escherichia coli* pose a serious global threat to public health.[1,2] Among these pathogens, *Salmonella* is particularly lethal and can lead to fatalities. Therefore, the urgent development of rapid and precise bacterial detection sensors is crucial to ensure food safety.

The enzyme-linked immunosorbent assay (ELISA)[3,4] and polymerase chain reaction (PCR)[5,6] are traditional culture methods that provide high detection sensitivity and accuracy. They can be automated and used for large-scale testing with suitable equipment and software. However, they require specialized technical expertise and specific knowledge of genes or antibodies, potentially restricting their applicability to certain targets. Moreover, the analysis process is time-consuming, presenting challenges for obtaining real-time results. Hence, surface plasmon resonance (SPR),[7–9] surface enhanced Raman scattering (SERS),[10–12] and electrochemical methods like electrochemical impedance spectroscopy (EIS)[13–15] or cyclic voltammetry (CV)[16–18] have been employed to expedite detection. These methods provide rapid responses and high sensitivity, enabling the detection of low concentrations of target substances. However, akin to traditional methods, they are constrained by the requirement for specialized equipment and the elevated cost of result verification. However, similar to conventional techniques, their utility is restricted by the necessity for specialized equipment and substantial expense of result verification.

In order to address these issues, multiple ongoing studies are currently developing colorimetric biosensors that use polydiacetylene (PDA) to enable visual detection.[19–21] PDA sensors display easily observable color changes, affordability, and versatile application potential, driving comprehensive research in this

[a] *Green and Sustainable Materials R&D Department, Korea Institute of Industrial Technology (KITECH), Republic of Korea. E-mail: kioks@kitech.re.kr*
[b] *Department of Chemical and Biomolecular Engineering, Yonsei University, Seodaemun-gu, Seoul, 03722, Republic of Korea*
[c] *Department of BioNano Technology, Gachon University, Seongnamdae-ro, Sujeong-gu, Seongnam, Gyeonggi, 13120, Republic of Korea*
[d] *Department of Green Process and System Engineering, Korea University of Science & Technology (UST), Cheonan, Chungnam 31056, Republic of Korea*

† Electronic supplementary information (ESI) available. See DOI: https://doi.org/10.1039/d3ma00840a

field. The polymerization of diacetylene (DA) to form PDA occurs through a photoreaction without the need for a chemical initiator, enabling the synthesis of high purity PDA without byproducts. The color characteristics of PDA arise from the π–π* absorption in the organized alternating ene–yne backbone.[22] Because of their amphiphilic nature, DA monomers will spontaneously arrange in a water-based solution due to the van der Waals interactions occurring among the hydrophobic alkyl chains.[23,24] Hence, when exposed to 254 nm UV irradiation, PDA supramolecules appear in blue. PDA, a conjugated polymer with distinct optical properties, is well-suited for creating color-changing and fluorescent sensors. It undergoes a chromatic transition from blue to red in response to external stimuli such as temperature,[25] pH,[26] light, organic solvents,[27] and receptor binding.[28] This color change is visually observable, cost-effective, and biocompatible. Interestingly, the PDA sensor can operate as a selective colorimetric sensor, detecting target substances with specificity.[29] This is accomplished through the functionalization of receptor entities (*e.g.*, ligands, lipids, aptamers, and antibodies) capable of recognizing specific substances, onto the surface of PDA liposomes. Among these, aptamers exhibit thermal stability and remarkable storage longevity due to their inherent chemical characteristics. Their cost-effectiveness and relative simplicity stem from their potential to chemically or enzymatically synthesize significant quantities of aptamers.[30] These advantages have led to the development of numerous aptamer-based analysis systems (aptasensors) for diverse applications, including food safety, environmental monitoring, and disease diagnostics.[31,32] Therefore, despite having a high detection limit, the PDA liposome–aptamer sensor demonstrates distinctiveness from existing *Salmonella* detection systems in that it allows for real-time confirmation of *Salmonella* concentrations at levels harmful to humans within a short period and visually. Moreover, it offers cost savings as it does not require specialized technical expertise and equipment.

In this study, we introduce a PDA-based liposome sensor capable of rapidly and accurately detecting *Salmonella via* a colorimetric response. The developed PDA liposome sensor is composed of a PDA liposome material surface-functionalized with an aptamer, a single-stranded DNA molecule exhibiting exceptional binding capability towards *Salmonella*. It is a notable achievement that the PDA liposome–aptamer sensor can detect *Salmonella* within less than 15 minutes through a colorimetric change observable to the naked eye. In contrast to previous intricate and time-intensive approaches, these results showcase a swift and straightforward real-time method for detecting foodborne pathogens like *Salmonella*, devoid of costly equipment or intricate preprocessing. These results demonstrate promising potential of sensor materials that can be extensively utilized in practical applications.

2. Experimental methods

2.1. Materials

10,12-Tricosadiynoic acid (TCDA, ≥98%), *N*-hydroxysuccinimide (NHS, 98%), *N*-(3-dimethylaminopropyl)-*N*′-ethylcarbodiimide hydrochloride (EDC-HCl), 1,2-dimyristoyl-*sn-glycero*-3-phosphocholine (DMPC), chloroform (ACS reagent, ≥99.8%), ethanolamine (≥98%) and potassium bromide (KBr, Fourier transform infrared (FTIR) grade, ≥99%) were purchased from Sigma-Aldrich. 2-[4-(2-hydroxyethyl)piperazin-1-yl]ethanesulfonic acid (HEPES, pH 7.0) was purchased from Biosolution. The ssDNA sequences (/5AmMC12/AGT AAT GCC CGG TAG TTA TTC AAA GAT GAG TAG GAA AAG A) were sourced from Integrated DNA Technologies (IDT).

2.2. Synthesis of NHS-modified diacetylene monomers (TCDA-NHS)

TCDA-NHS monomers were synthesized following a previously reported method.[33] 10,12-Tricosadiynoic acid (TCDA, 0.72 mmol, 0.25 g), *N*-(3-dimethylaminopropyl)-*N*′-ethylcarbodiimide hydrochloride (EDC-HCl 1.35 mmol, 0.26 g) and *N*-hydroxysuccinimide (NHS, 1.07 mmol, 0.12 g) were dissolved in 4 mL of methylene chloride (Fig. S1, ESI†). The mixture was then stirred for 2 hours at room temperature. After the solution was evaporated using a rotary evaporator and the residue was purified by extraction with ethyl acetate, TCDA-NHS monomers were obtained as a white solid. The chemical structure of TCDA-NHS was confirmed by using ^{1}H nuclear magnetic resonance (NMR, 300 MHz, chloroform-*d*, *δ*): ppm 2.85 (s, 4H), 2.61 (t, 2H), 2.25 (t, 4H), 1.79–1.26 (m, 28H), 0.89 (t, 3H).

2.3. Preparation of PDA liposomes conjugated with aptamers

PDA liposomes conjugated with aptamers were synthesized using the established batch method.[33] TCDA and TCDA-NHS were separately dissolved in chloroform in glass vials, and the solutions were combined in a 9 : 1 molar ratio of TCDA to TCDA-NHS. Following this, DMPC was added to the mixture solution at a 0.6 ratio and dissolved in chloroform to produce a 1 mM TCDA liposome solution. Next, the solution was filtered through a 0.2 μm syringe filter to eliminate any aggregated material or large particles. The solvent was then removed by nitrogen purging, resulting in a thin film on the flask's surface. Following this, 10 mL of deionized water was added to the flask. The solution was sonicated at 80 °C for 5 minutes until a translucent cloudy suspension was achieved. Subsequently, the solution was gradually cooled to room temperature and stored at 4 °C overnight. A 1% aptamer solution was conjugated to the liposome surface by 4-hour agitation. 0.13 mol of ethanolamine was added to inactivate the remaining unreacted NHS. To make an optically active PDA liposome, the PDA liposome–aptamer solution was exposed to UV light at 254 nm for approximately 30 minutes, during which the milky solution transformed into a blue colored solution by forming a conjugated backbone structure with an alternating ene–yne (C=C and C≡C).

2.4. Characterization

2.4.1. Fourier transform infrared (FT-IR) spectroscopy. Transmittance mode FT-IR analysis was conducted on a PDA liposome and a liposome with an attached aptamer. Samples for IR analysis were prepared by freeze-drying the solution samples. Each dried sample was analyzed using a KBr pellet (PDA liposome/PDA liposome–aptamer:KBr ratio = 1 : 100).

The FTIR spectra were acquired through transmission measurements across a scanning range of 3600–600 cm^{-1}, with a resolution of 2 cm^{-1} and 16 scans.

2.4.2. UV-Vis spectroscopy. To evaluate the efficiency of the attached aptamers, a UV absorbance assay was conducted on the liposomes. Prior to the assay, dialysis was employed to eliminate unreacted aptamers from the liposome samples. The liposome–aptamer solution was subsequently introduced into dialysis tubes (Biotech CE tubing with MWCO 100–500 D, USA). The tube was placed in a beaker with a volume of 5 L and dialyzed against water for minimum 72 hours. The water was exchanged three times within this time range. UV-Vis spectroscopy (Shimadzu, UV-1800) was performed at room temperature, covering a wavelength range from 500 nm to 700 nm.

2.4.3. Raman scattering. After dialyzing the blue, purple and red phase solutions, the samples were converted into powdered forms and then subjected to Raman spectroscopy measurements. The Raman spectra were recorded using a LabRAM HR Evolution Visible_NIR (HORIBA) Raman system with a 633 nm laser excitation source.

2.4.4. Particle size analysis (PSA). Particle size analysis was performed using a Particle Size Analyzer (Otsuka Electronics, ELSZ-2000ZS) to ascertain the dimensions of PDA liposomes and PDA liposome–aptamers.

2.4.5. Fluorescence spectroscopy. Fluorescence spectra were recorded utilizing photoluminescence (PerkinElmer, LS 55) to detect diverse *Salmonella* concentrations. The fluorescence spectrum was recorded at an excitation wavelength of 270 nm, recording the maximum fluorescence level of the sample.

2.4.6. Colorimetric assays for *S. typhimurium* and sensitivity and linearity tests. *S. typhimurium* (LB medium, 37 °C, Korea), *Saccharomyces cerevisiae* (YPD 2% medium, 30 °C, Korea), and *Corynebacterium glutamicum* (BHI medium, 30 °C, Korea) were incubated in a shaking incubator at 250 rpm overnight. 1 mL of each incubate (OD_{600} of 1) was centrifuged at 13 000 rpm for 1 minute and the supernatant was removed. For cell lysis, the cell pellet from each incubation was resuspended in 4 mL of B-PER® Bacterial Protein Extraction Reagent per 1 g of cell weight and left to react at room temperature for 10–15 minutes. Subsequently, the lysed bacteria were gradually diluted to a concentration range of 1×10 CFU mL^{-1} to 1×10^7 CFU mL^{-1} using 100 mM HEPES buffer. The final concentration of PDA liposomes was adjusted to 0.1 mM by mixing 300 μL of 1 mM PDA solution with 2700 μL of standard *Salmonella* solution diluted to the specified concentration. At a *Salmonella* concentration of 10^4 CFU mL^{-1}, we monitored color changes and UV-visible spectra every 15 minutes for 60 minutes at 37 °C to track alterations in color and CR values over time. To assess the sensitivity and linearity of the PDA liposome–aptamer sensor, we varied the *Salmonella* concentration from 0 CFU mL^{-1} to 10^7 CFU mL^{-1}. CR values for different *Salmonella* concentrations were determined with a 15-minute incubation time.

2.4.7. Detection of *S. typhimurium* in food samples. In the investigation of the presence of *S. typhimurium* in food samples, a white egg served as the chosen food matrix. The procedures for preparing the food samples and introducing bacterial spiking were adopted from a previous paper.[34] Egg white (1 g) was mixed with 9 mL HEPES solution (100 mM) and homogenized thoroughly. Subsequently, the mixture underwent centrifugation at 10 000 rpm for 10 minutes to eliminate any solid impurities in the egg white. Bacteria in the resulting supernatant were filtered using a 0.22 μm pore size filter. To examine the impact of the food matrix on the detection of *S. typhimurium*, a solution comprising 1 mL of the food matrix and 1 mL of the bacterial solution was prepared, and the volume was adjusted to 10 mL with a 100 mM HEPES buffer. Then, PDA liposome–aptamer sensor solutions were applied to capture *S. typhimurium* from real samples. The following operations were the same as those described in Section 2.4.6.

3. Results and discussion

3.1. Mechanism of colorimetric detection of *Salmonella*

Fig. 1 demonstrates the fabrication and sensing mechanism of the PDA liposome sensor material, enabling swift visual *Salmonella* detection. Polydiacetylene (PDA) monomers, bearing double and triple bonds, self-assemble into bilipid liposomes.[35] UV or γ irradiation prompts the creation of an alternating ene–yne conjugated polymer backbone chain in PDA through 1,4-addition. As a consequence of the optical π–π* absorption of the polymer main chain, the resulting PDA exhibits a blue color with a maximum wavelength (λ_{max}) of 640 nm.[36,37] Different stimuli like temperature,[25] pH,[26] mechanical stress, or chemical bonding[38] cause the blue PDA liposome to experience an energy gap increase between overlapping p-orbitals. This leads to an absorption spectrum expansion in the conjugated backbone, inducing a distinct color shift from blue to red with a maximum wavelength (λ_{max}) of 550 nm.

We engineered PDA-based liposomes with high-specificity aptamers to selectively bind to bacteria and pathogens. The nano-sized PDA vesicle was activated by *N*-hydroxysuccinimide (NHS) and *N*-(3-dimethylaminopropyl)-*N*′-ethylcarbodiimide hydrochloride (EDC-HCl) to form a reactive intermediate. The carboxyl group of the PDA vesicle and the amino group of the aptamer underwent peptide bonding, leading to the synthesis of PDA liposome–aptamer. After incorporating a *Salmonella*-specific single-stranded DNA aptamer onto the PDA liposomes, in an environment where bacteria are present, the bacteria specifically bind to the aptamer surface. The distorted conjugated backbone of the PDA liposome, induced by external stimuli, exhibits a visible color change from blue to red. Through this process, *Salmonella* can be easily and straightforwardly detected. The DNA sequence of the *Salmonella*-specific aptamer was AGT AAT GCC CGG TAG TTA TTC AAA GAT GAG TAG GAA AAG A, which was selected based on previous work.[39] The aptamer sensor provides confirmation of *Salmonella* detection through molecular recognition and conformational changes in the PDA–liposome structure.

In this study, the PDA monomer used was 10,12-tricosadiynoic acid (TCDA). In addition, TCDA-NHS was employed as a co-monomer to achieve surface modification of liposomes with

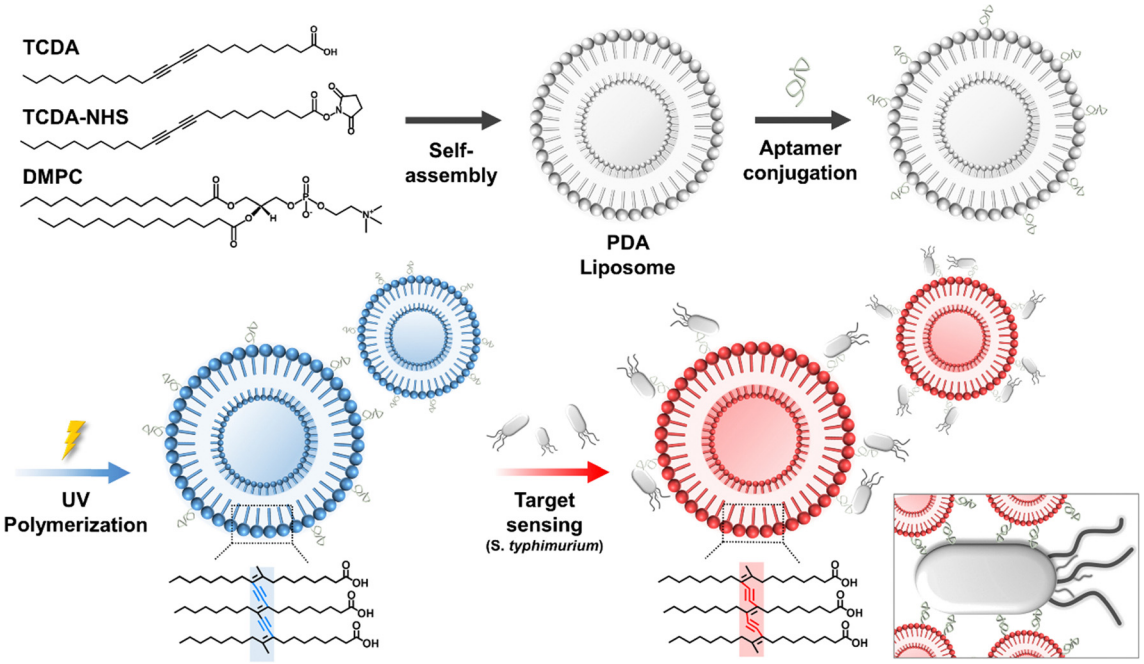

Fig. 1 Schematic of the fabrication of the PDA liposome–aptamer sensor for *Salmonella typhimurium* detection.

aptamers, wherein the NHS functional group of TCDA facilitated the formation of amide bonds with amine-terminated aptamers, thus enhancing the functionalization of the liposome surface. To enhance the structural flexibility of the liposomes and improve sensing sensitivity, the phospholipid 1,2-dimyristoyl-*sn-glycero*-3-phosphocholine (DMPC) was included. In the initial experimental phase, we investigated different DA monomers, phospholipid varieties and composition ratios. To simplify the experimental process, we chose liposome compositions based on assessing the thermal colorimetric response properties of various liposome components and ratios without incorporating aptamers (see Table S1, ESI†). The resulting optimal liposome composition was determined to be TCDA : TCDA-NHS : DMPC in a molar ratio of 0.9 : 0.1 : 0.6 and was prepared using an established water bath method.[33] These three components (TCDA, TCDA-NHS, and DMPC) self-assembled to form liposomes with a bilipid structure, as depicted in Fig. 1. The aminated aptamer was functionalized on the liposome surface by forming an amide bond with the NHS group of the TCDA-NHS. A blue PDA–liposome aptamer sensor was prepared successfully by sequentially conjugating the aptamer and undergoing UV polymerization processes.

3.2. Characterization of the PDA liposome–aptamer sensor

Fig. 2 shows the results of the structural analysis of the successfully prepared liposomes. To validate the successful conjugation of the aminated aptamer onto the liposome surface using the aforementioned method, we examined the UV-Vis and FT-IR spectra of liposome samples before and after aptamer attachment. Unconjugated aptamers were previously eliminated through dialysis.

Fig. 2a illustrates the FT-IR spectra of a liposome and a liposome conjugated with an aptamer. The characteristic peaks for the carboxylic acid of TCDA appeared at 3430 cm^{-1} (O–H stretching) and 1737 cm^{-1} (C═O stretching). The characteristic peak of the phospholipid was identified at 1074 cm^{-1} (PO_2 asymmetric vibration). The amine group of the aptamer reacts with the carboxylic acid (–COOH) of TCDA, resulting in the formation of an amide bond. The presence of these amide bonds is confirmed by the characteristic peaks observed at 3397 cm^{-1} and 3207 cm^{-1} (N–H stretching), 1650 cm^{-1} (C═O stretching), and 1535 cm^{-1} (in-plane N–H bending) in the FT-IR spectrum of the liposome–aptamer sample. These results demonstrate the successful chemical conjugation of the aptamer to the PDA–liposome.

In addition, the conjugation between liposomes and aptamers can also be confirmed by UV-Vis spectral investigation (Fig. 2b). The aptamer used in this study is a single-stranded DNA comprised of the four nucleotide bases: guanine (G), cytosine (C), adenine (A), and thymine (T). The aromatic rings within the purine and pyrimidine structures of guanine, cytosine, adenine, and thymine have absorbance in the 260 nm region (Fig. S2, ESI†).[40] As depicted in Fig. 2b, aptamer-conjugated liposomes (PDA liposome–aptamer) have a high absorbance at 260 nm, a characteristic peak attributed to the aptamer nucleotide. The UV-Vis spectra were employed to quantitatively determine the conjugation efficiency of the aptamer to the liposome. This determination involves correlating the attached aptamer amount with the initially fed aptamer quantity by measuring the absorbance at 260 nm and comparing it to the aptamer concentration in the standard sample. Fig. 2c demonstrates the modulation of aptamer concentration in relation to the PDA monomer, ranging from 1 to 12 mol% (Fig. S3, ESI†). Notably, the aptamer consistently exhibited a chemical binding efficiency of approximately 80% relative to its initial introduced content in all instances. A PDA

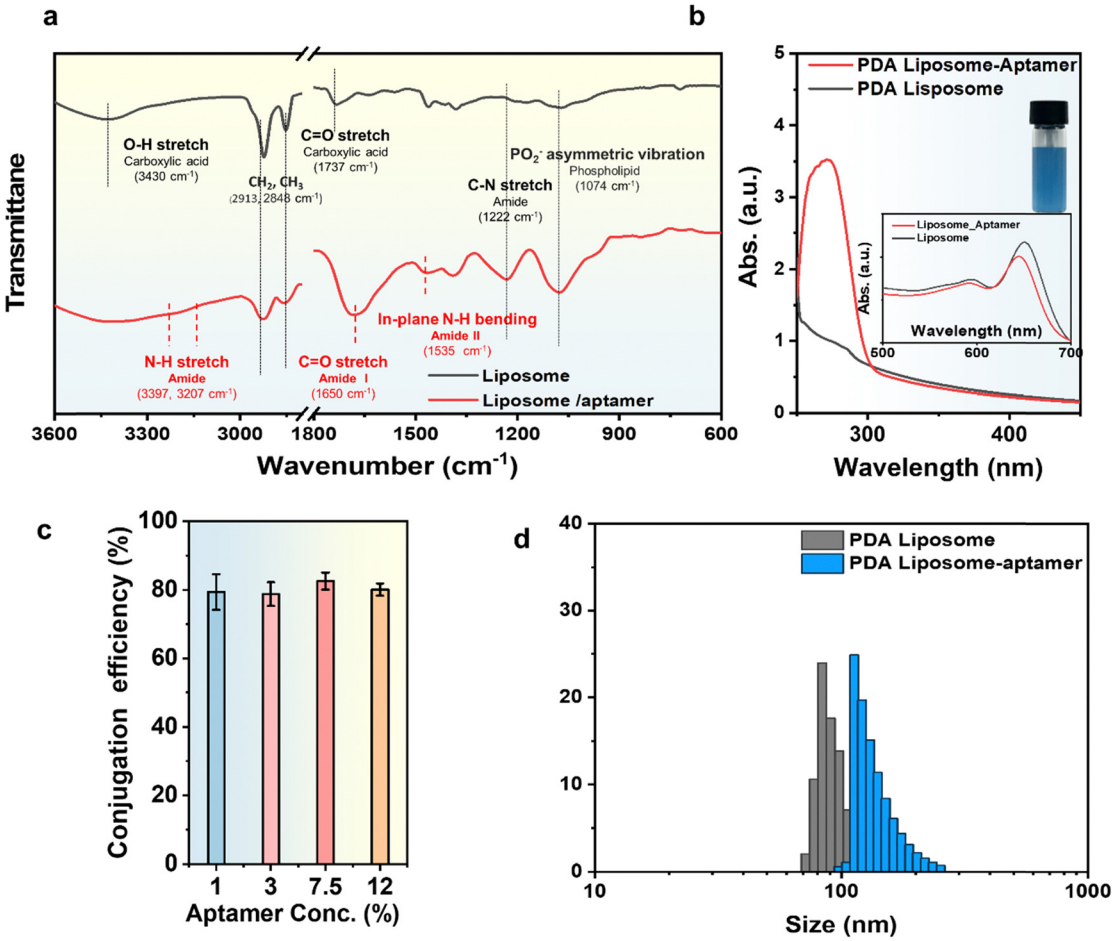

Fig. 2 (a) FT-IR peak alterations resulting from PDA liposome and aptamer binding. (b) UV-Vis spectrum illustrating the aptamer conjugation onto the surface of liposomes. (c) Aptamer conjugation efficiency to PDA monomers. (d) Size distribution change of initial PDA vesicles (black) and PDA liposomes conjugated with aptamers (blue).

liposome–aptamer with 1% aptamer concentration was selected as the sensor material, as attaching aptamer concentrations exceeding 3% to PDA liposomes led to reduced polymerization efficiency. Fig. 2d presents the results of particle size analysis (PSA), validating the size of liposomes prepared using the mentioned bath method. The initial size of the PDA liposome was determined to be approximately 100 nm. After aptamer conjugation, the size of the liposome particles slightly increased to around 137 nm. This outcome is attributed to the presence of an extra hydrophilic molecule.

3.3. Feasibility of *Salmonella* detection

The developed PDA–aptamer liposomal sensor material possesses characteristics that enable the naked-eye detection of *Salmonella* within 15 minutes through a rapid and precise colorimetric reaction. Fig. 3 illustrates that the PDA liposome–aptamer sensor, loaded with *Salmonella* at a concentration of 1×10^4 CFU mL^{-1}, undergoes a rapid visible color transition from blue to purple within 15 minutes. Furthermore, after 45 minutes, the sensor material transforms into a deep pink color. This change can be attributed to the fact that binding of a *Salmonella*-specific aptamer to *Salmonella* triggers surface interaction, leading to a conformational change in the PDA-conjugated chain and resulting in a color shift from blue to red.[41]

UV-Vis spectrum measurements were performed over sensing time to investigate the alterations in optical properties within the PDA liposome–aptamer resulting from the introduction of *Salmonella* at a concentration of 1×10^4 CFU mL^{-1}. Upon adding *Salmonella* to the prepared PDA liposome–aptamer solution, a gradual decrease in absorption in the 640 nm region and an increase in absorption in the 547 nm region were observed over time (Fig. 3a and b), indicating a typical blue-to-red transition of the PDA liposome–aptamer. As illustrated in Fig. 3b, during the initial phase ($t < 15$ min), the absorption at 640 nm diminished while the absorption at 547 nm simultaneously increased. A pronounced color alteration became apparent at the 15-minute mark. Additionally, at the 60-minute interval, the absorption peaks at 640 and 547 nm reached their zenith.

The quantitative assessment of changes in the absorbance spectrum can be determined by the colorimetric response (CR) value calculated as follows:

$$\mathrm{CR}\ (\%) = \frac{\mathrm{PB}_0 - \mathrm{PB}_1}{\mathrm{PB}_0} \times 100,\ \mathrm{PB} = \frac{A_{640\mathrm{nm}}}{(A_{640\mathrm{nm}} + A_{547\mathrm{nm}})}$$

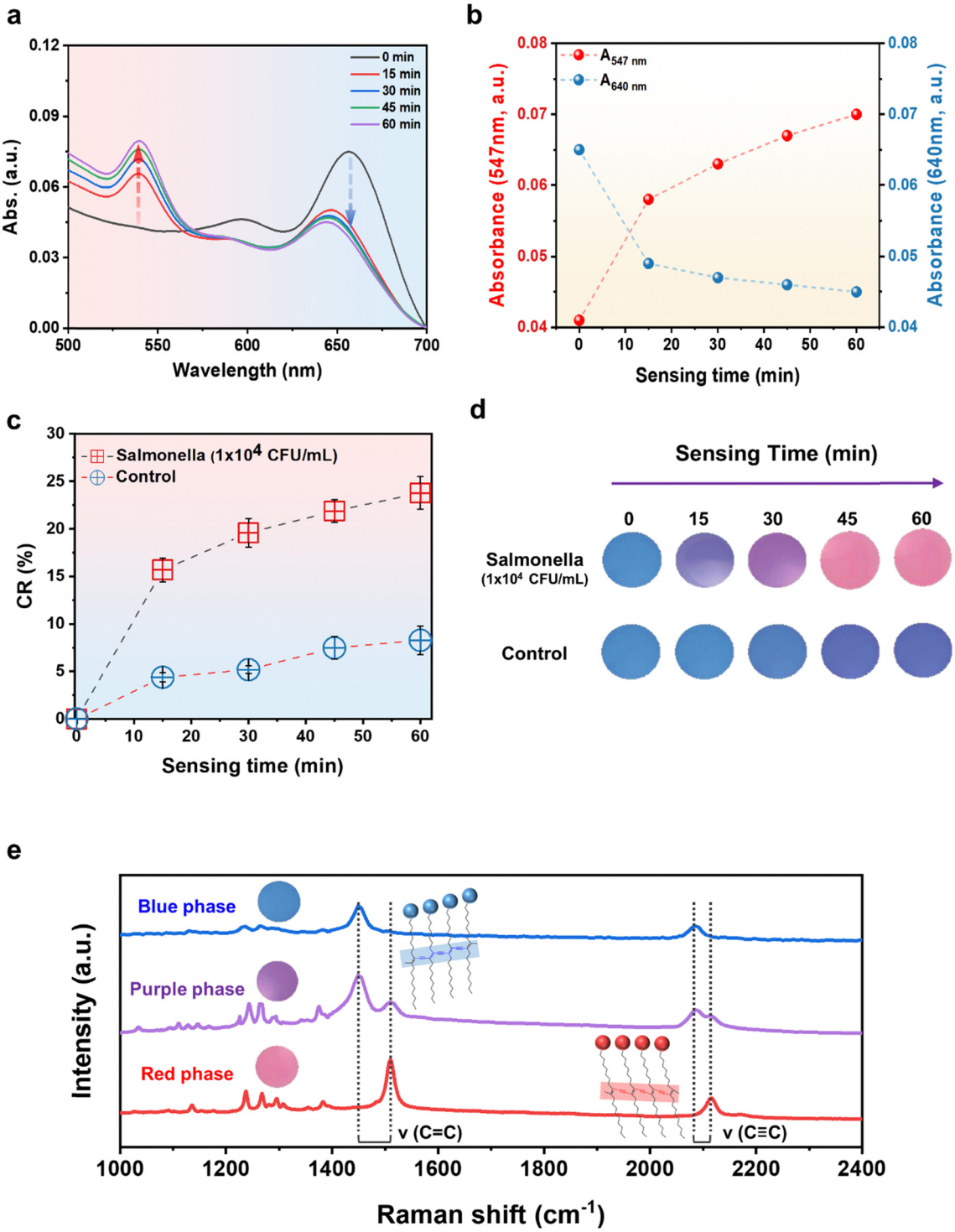

Fig. 3 (a) UV-Vis absorption spectra of the PDA liposome–aptamer sensor at a *Salmonella* concentration of 1×10^4 CFU mL^{-1} for 1 hour. (b) Absorption plots as a function of time at 640 nm and 547 nm. (c) Colorimetric responses of the PDA liposome–aptamer sensor with a *Salmonella* concentration of 1×10^4 CFU mL^{-1} along with (d) a photograph of the resulting color change. (e) Raman spectra corresponding to the blue-phase, purple-phase, and red-phase of the PDA liposome–aptamer sensor.

A_{640nm} and A_{547nm} in the UV-Vis spectrum correspond to the absorbance at 640 nm and 547 nm, respectively. PB_0 denotes the initial value of the *Salmonella* and PDA liposome–aptamer sensor mixture, and PB_1 represents the value measured after a certain time. A higher CR (%) value indicates a more efficient conversion to red color.

Fig. 3c and d demonstrates the clear color change of the sample, turning purple at 15 minutes and pink at 45 minutes,

with corresponding CR values of 15.7% and 21.9%, respectively. A CR value of 7–8% or higher is commonly considered to be a value that can clearly distinguish the color change with the naked eye; the CR value of the PDA liposome–aptamer sensor exceeds 15.7% within 15 minutes, which indicates a high detection efficiency of *Salmonella* Interestingly, the control condition with a *Salmonella* concentration of 0 CFU mL^{-1} shows no significant color change in the PDA liposome–aptamer material after 30 minutes, maintaining its initial blue color, with color changes contributing to less than 6% CR value (Fig. 3d). However, for a more accurate comparison, it is recommended to consider color changes occurring within 30 minutes, as the CR value of the control sample reaches 8.3% at 60 minutes. These results hold significance as they allow for quick and easy confirmation of the presence of *Salmonella* using naked-eye observation. This approach contrasts with conventional detection methods that are known for their complexity and time-consuming nature.[3]

As shown in Fig. 3e, the blue-to-red chromatic transition of the PDA liposome was confirmed using Raman spectroscopy with a laser excitation wavelength of 633 nm. In the blue phase, two bands associated with the conjugated alkyne–alkene structure were observed at 2082 cm^{-1} (C≡C) and 1450 cm^{-1} (C=C) in the PDA liposome–aptamer. The Raman spectrum of the purple phase PDA liposome–aptamer material, after 15 minutes of inoculation with *Salmonella* (1×10^4 CFU mL^{-1}), revealed a partial shift of the alkyne–alkene band to higher frequencies at 2122 cm^{-1} and 1817 cm^{-1}, indicating a partial distortion of the conjugated yne–ene chain. However, the red phase, which was exposed to *Salmonella* for a longer period (45 minutes), displays a notable upward shift of the alkyne–alkene band to higher frequencies, which demonstrates that the increased binding of numerous *Salmonella* fragments to the aptamer leads to the full distortion of the conjugated yne–ene chain.

As mentioned earlier, we selected a *Salmonella*-specific aptamer (sequence: AGTAATGCC CGGTAGTTATTCAAAGATG AGTAGGAAAAGA) for this experiment based on previously reported papers.[39] As shown in the above experiment, the PDA liposome–aptamer sensor confirmed a clear colorimetric reaction from blue to red of the PDA liposome material through the specific binding of the aptamer to *Salmonella*. Comparative experiments were performed to investigate the function of *Salmonella*-selective aptamers in PDA liposome sensors (see Fig. S4, ESI†). For the purpose of comparison, we categorized liposomal materials into three types. Type 1 liposomes, lacking aptamer functionalization, and type 3 liposomes, possessing non-*Salmonella*-specific aptamers, do not exhibit a specific colorimetric response to *Salmonella*. Conversely, type 2, equipped with *Salmonella*-specific aptamers, demonstrates a noticeable color alteration in the presence of *Salmonella*. These experimental findings reveal that the particular colorimetric reaction of the PDA liposome–aptamer sensor to *Salmonella* results from the specific interaction between the aptamer and *Salmonella*.

3.4. Sensitivity and limit of detection (LOD) range

Next, we focused our attention towards evaluating the PDA liposome–aptamer and its chromatic transition properties in response to changing *Salmonella* concentrations. PDA liposome–aptamer solutions were exposed to different concentrations of *S. typhimurium*, ranging from 1×10^1 CFU mL^{-1} to 1×10^7 CFU mL^{-1}, for a duration of 15 minutes at 37 °C. To monitor the blue-to-red transition upon addition of *Salmonella*, we recorded the UV-Vis spectrum of each sample (Fig. 4a). As anticipated, the introduction of *Salmonella* results in a characteristic blue-to-red color transition, which becomes more pronounced with higher concentrations of *Salmonella*. In Fig. 4b, an excellent linear correlation between CR% and *Salmonella* concentration is observed within the range of 1×10^3 CFU mL^{-1} to 1×10^7 CFU mL^{-1}, with a linear response described by the equation $y = 3.32x + 2.76$ ($R^2 = 0.99$). Based on this correlation curve, it is evident that quantitative analysis of an unknown *Salmonella* concentration is achievable.

A photograph of a PDA liposome–aptamer solution exposed to different concentrations of *Salmonella* during a 15-minute incubation at 37 °C is shown in Fig. 4c. A noticeable color change, although subtle, in comparison to the control, is evident at *Salmonella* concentrations as low as 1×10^3 CFU mL^{-1}. Furthermore, concentrations surpassing 1×10^4 CFU mL^{-1} display a distinct and substantial color change. These results indicate that the limit of detection (LOD) for *Salmonella* on the prepared PDA liposome–aptamer sensor is 1×10^3 CFU mL^{-1}, which is comparable to the lowest value of the visual detection limit in a previously reported study on *Salmonella* detection sensors.[42,43] The detection capability of the PDA liposome sensor is highly significant as it enables the naked-eye identification of *Salmonella* at concentrations above 1×10^3 CFU mL^{-1}, which is reported as a human health hazard,[44] within a rapid timeframe of 15 minutes.

The conjugated backbone of PDA liposomes, distorted by external stimuli, is known to exhibit strong fluorescent properties in addition to the well-known blue-to-red color change. We observed the fluorescence properties of PDA liposome–aptamer sensors exposed to various concentrations of *Salmonella* for a duration of 15 minutes at 37 °C (Fig. 4d).

As expected, the PDA liposome–aptamer emitted strong fluorescence at 550 nm with increasing *Salmonella* concentration. The fluorescence intensity of the PDA liposome–aptamer was also plotted against the *Salmonella* concentration (Fig. 4e). A linear correlation ($R^2 = 0.92$) was obtained over the concentration range of 1×10^1–1×10^7 CFU mL^{-1}.

3.5. Detection of *S. typhimurium* in eggs and recovery

In order to evaluate the feasibility of the sensor, *Salmonella* in actual food samples was detected using a PDA liposome–aptamer sensor. Fig. 5a shows the general procedure for food sample treatment and the sensing procedure. An egg white served as the food matrix and various concentrations of *Salmonella* (10^3, 10^4, 10^5, 10^6, and 10^7 CFU mL^{-1}) were spiked. The procedures for preparing the food matrix and bacterial spiking were adopted from a previous paper.[34] Then, PDA liposome–aptamer sensor solutions were applied to capture *S. typhimurium* from real samples at 37 °C for 15 minutes and the color change was monitored. Fig. 5b shows the recovery and

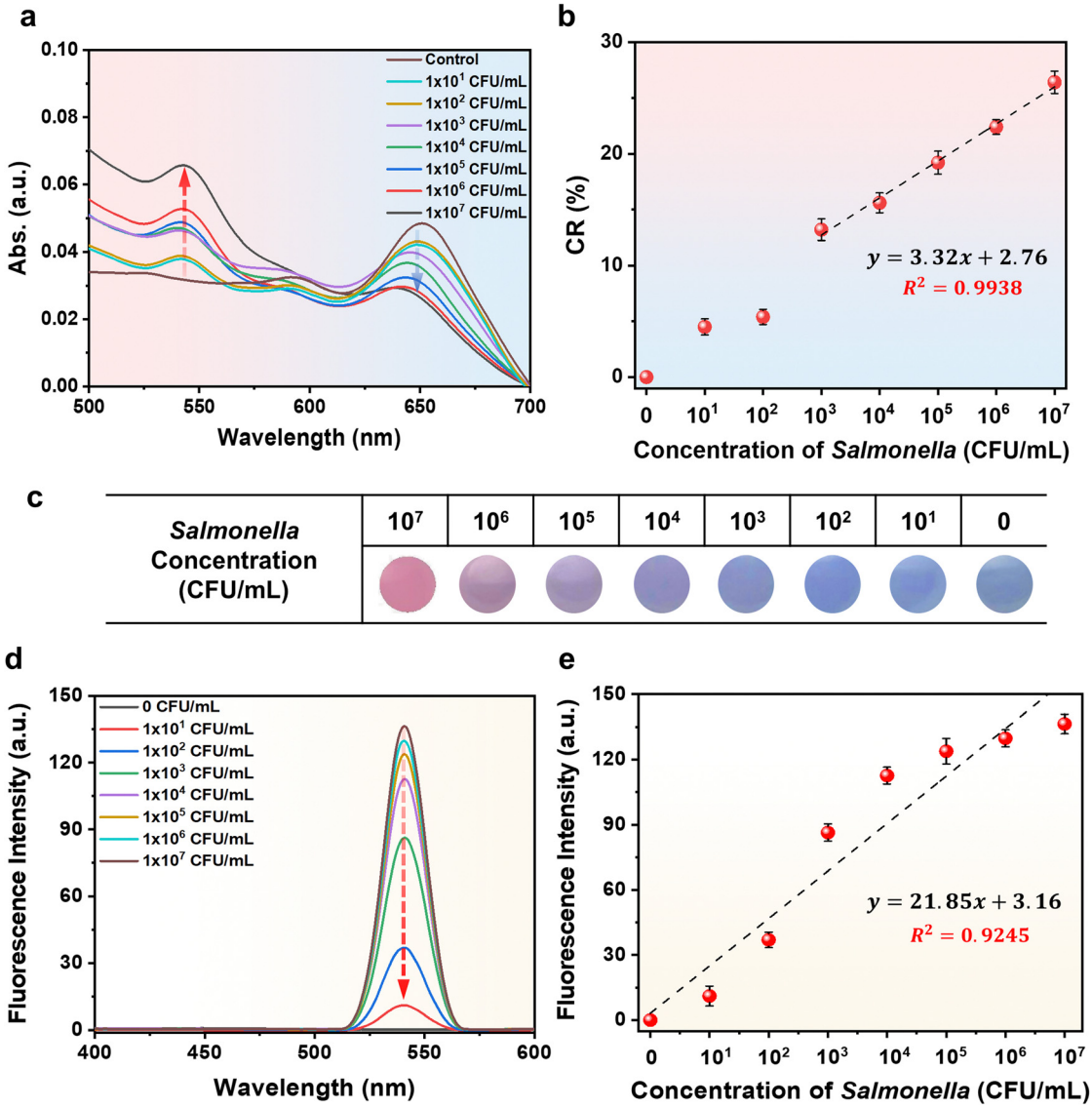

Fig. 4 (a) UV-Vis absorption spectra for various *Salmonella* concentrations ranging from 1×10 to 1×10^7 CFU mL^{-1}. (b) Calibration curve and linearity results for CR% values after 15 minutes of exposure to different concentrations of *Salmonella*. (c) Photographs depicting color changes of PDA liposome–aptamer solution after 15 minutes of exposure to different concentrations of *Salmonella*. (d) Fluorescence spectra for different *Salmonella* concentrations from 1×10 to 1×10^7 CFU mL^{-1}. (e) Calibration curve and linearity results for fluorescence intensity after 15 minutes of exposure to different *Salmonella* concentrations.

coefficient of variation (CV) of the PDA liposome–aptamer sensor in the food matrix. The recoveries from all samples range from 91.32 to 107.97%. The recoveries for each sample were achieved as follows: 91.32% for 10^3 CFU mL^{-1}, 103.15% for 10^4 CFU mL^{-1}, 91.76% for 10^5 CFU mL^{-1}, 107.97% for 10^6 CFU mL^{-1}, and 97.36% for 10^7 CFU mL^{-1} *Salmonella*. The reproducibility of the PDA liposome–aptamer sensor was also evaluated by measuring its response to *Salmonella* concentrations ranging from 10^3 to 10^7 CFU mL^{-1}. The repeatability of the sensor was measured three times independently under the same working conditions, and the coefficient of variation (CV) values for concentrations of 10^3, 10^4, 10^5, 10^6, and 10^7 CFU mL^{-1} were calculated to be 0.98%, 2.10%, 1.25%, 1.56% and 3.01%, respectively. The above results demonstrate the high reproducibility and repeatability of the sensor we have developed. In addition to the colorimetric response, strong fluorescence characteristics of the PDA liposome–aptamer sensor were also observed in authentic food samples (Fig. S5, ESI†).

To assess the specificity of the PDA liposome–aptamer sensor for *S. typhimurium*, we examined its response to different strains, including *S. typhimurium*, *E. coli*, *S. cerevisiae*, and *C. glutamicum*. The sensing characteristics of the PDA liposome–aptamer for each strain were assessed by incubation at 37 °C for 15 minutes with a concentration of 1×10^4 CFU mL^{-1} and the CR values were determined using a previously described method. As depicted in Fig. 5c, the prepared PDA liposome–aptamer sensor demonstrates a markedly elevated CR value (15.3%) for *S. typhimurium*, in contrast to the other

a

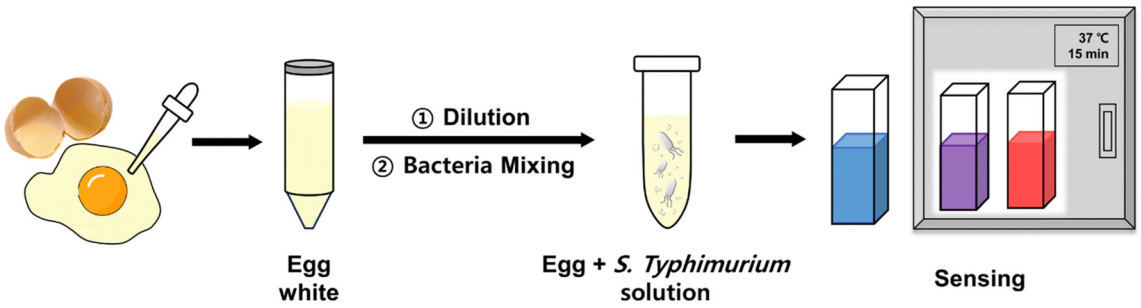

b

Sample	Spiked *Salmonella* (Log_{10} CFU/mL)	[a]Tested *Salmonella* (Log_{10} CFU/mL)	[b]Recovery (%)	[c]CV (%)
Egg-derived solution	7	6.82	97.36	0.98
	6	6.48	107.97	2.10
	5	4.59	91.76	1.25
	4	4.13	103.15	1.56
	3	2.74	91.32	3.01

[a] Mean value of three independent measurements
[b] Tested value/expected value × 100
[c] Coefficient of variation (CV) = (SD/mean) × 100

c

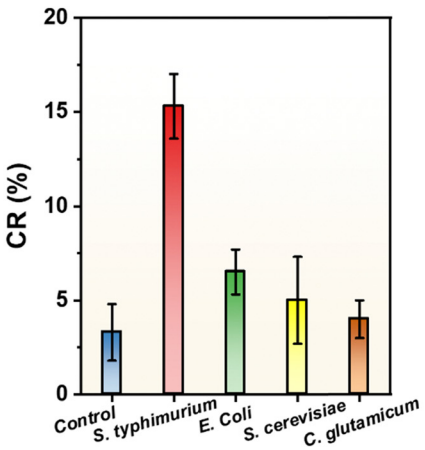

Fig. 5 (a) Detection of *Salmonella* in actual food samples (eggs). (b) The recovery rate of *Salmonella* in egg samples. (c) Specificity of the PDA liposome–aptamer sensor for detection of *Salmonella* among various bacteria (concentration of all bacteria was 1×10^4 CFU mL^{-1}).

experimental groups with CR values below 7%. Notably, the resemblance of the CR values for *S. cerevisiae* and *C. glutamicum* to those of the control samples implies that the PDA liposome–aptamer sensors have a distinct color response to *S. typhimurium*. These results can be attributed to the unique ability of the aptamers to specifically bind to *Salmonella*. Furthermore, the PDA–liposome aptamer sensor material exhibits a discriminating and enhanced colorimetric reaction to *Salmonella* when compared to *E. coli*, a common bacterium that could be found in food samples. Remarkably, this specificity is visually confirmable, unequivocally

Table 1 Comparison of various techniques for *Salmonella* detection sensors

Detection techniques	Detection method	Detection time	Materials	Linear detection range (CFU mL^{-1})	Limit of detection (CFU mL^{-1})	Ref.
PCR	qPCR	Several days		—	—	5
ELISA	Microplate reader	24 hours		1.4×10^5	—	3
SPR	SPR assay	4 hours		3.2×10^4–10^7	5.0×10^4	7
SERS	Raman	—	—	1.0×10^3–10^7	15	10
Electrochemical detecting	EIS, CV	1 hour		1.0×10^2–10^6	5.0×10^2	13
	EIS	2 hours		1.0×10 –10^8	80	14
	DPV	1 hour		1.0×10–10^8	10	16
	DPV	2 hours		9.6×1–10^3	8.1	17
Colorimetric	Naked-eye	5 hours	DNAzyme probe self-assembled GN	3.0×10^3 –10^6	3.0×10^3	40
	Naked-eye	48 hours	PCDA/SPH/CHO/Lysine	1.0×1–10^8	10	41
	Naked-eye	15 min	PDA liposome/aptamer	1.0×10^3 –10^7	1.0×10^3	This work

validating the sensitive and precise *Salmonella* detection achieved by the PDA liposome–aptamer sensor.

Table 1 summarizes and contrasts the attributes of various *Salmonella* detection sensors, including our newly devised PDA sensor. The PDA liposome–aptamer sensor demonstrates a rapid detection time of 15 minutes, markedly shorter than those of traditional techniques like PCR[5] and ELISA.[3] Furthermore, distinct from SPR,[7] SERS,[10] and electrochemical methods[13,14,16,17] requiring costly apparatus, our sensor uniquely detects *Salmonella* at concentrations surpassing 1×10^3 CFU mL^{-1}, a level hazardous to humans, within a 15-minute timeframe through direct visual assessment, notwithstanding its relatively higher detection threshold. Our novel devised PDA liposome–aptamer sensor enables naked-eye *Salmonella* detection within a brief timeframe (15 minutes), contrasting with earlier colorimetric approaches (5 hours for a DNAzyme-decorated gold nanoparticle sensor[45] and 48 hours for a PCDA/SPH/CHO/Lysine sensor[46]). Consequently, the *Salmonella*-specific PDA liposome–aptamer sensor holds significant potential for swift visual *Salmonella* detection.

4. Conclusions

We have successfully engineered a colorimetric biosensor with the capability to rapidly detect *Salmonella* through direct visual observation. The material composition of this biosensor was meticulously formulated by creating liposomes *via* the combination of TCDA:TCDA-NHS:DMPC, followed by a process of aptamer surface functionalization and subsequent UV polymerization, resulting in an affinity specifically tailored for *Salmonella* recognition. The synthesized biosensor framework showcases multiple advantageous aspects compared to established *Salmonella* detection methodologies and alternative sensing paradigms.

Foremost, the facile synthesis of both PDA liposomes and aptamers in considerable quantities presents a cost-effective and straightforward strategy for biosensor fabrication. Furthermore, the biosensor exhibited a distinct color transformation (CR: 25% for 1×10^4 CFU mL^{-1}) within a rapid 15-minute window at a temperature of 37 °C. Additionally, a linear correlation of CR values was observed across a spectrum of *Salmonella* concentrations. Impressively, *Salmonella* concentrations surpassing 1×10^3 CFU mL^{-1} were visibly detectable without the necessity for sophisticated analytical instrumentation. Concurrently, we have successfully demonstrated the biosensor's efficacy in detecting *Salmonella* in authentic food samples, thus underscoring the sensor's adaptability and its potential relevance in everyday scenarios.

Collectively, these empirical observations substantiate the biosensor's effectiveness and accessibility in detecting the pathogenic bacterium *Salmonella*, with the prospective capacity to significantly impact public health. Subsequent research efforts could focus on refining and optimizing the *Salmonella* detection approach, potentially encompassing the development of paper-based sensor arrays or the conception of user-friendly film-based kit configurations.

Conflicts of interest

There are no conflicts to declare.

Acknowledgements

This work was supported by the Big Issue Program (PEO24030) of the Korea Institute of Industrial Technology (KITECH), Republic of Korea.

References

1 R. V. Tauxe, *Emerging Infect. Dis.*, 1997, **3**, 425–434.
2 S. Finstad, C. A. O'Bryan, J. A. Marcy, P. G. Crandall and S. C. Ricke, *Food Res. Int.*, 2012, **45**, 789–794.
3 Y. He, Y. Ren, B. Guo, Y. Yang, Y. Ji, D. Zhang, J. Wang, Y. Wang and H. Wang, *Food Chem.*, 2020, **25**, 125942.
4 L. P. Mansfield and S. J. Forsythe, *Food Microbiol.*, 2001, **18**, 361–366.
5 M. Siala, A. Barbana, S. Smaoui, S. Hachicha, C. Marouane, S. Kammoun, R. Gdoura and F. Messadi-Akrout, *Front. Microbiol.*, 2017, **8**, 1–10.
6 D. De Medici, L. Croci, E. Delibato, S. Di Pasquale, E. Filetici and L. Toti, *Appl. Environ. Microbiol.*, 2003, **69**, 3456–3461.
7 D. Bhandari, F.-C. Chen and R. C. Bridgman, *Sensors*, 2022, **22**, 475.
8 B. K. Oh, Y. K. Kim, K. W. Park, W. H. Lee and J. W. Choi, *Biosens. Bioelectron.*, 2004, **19**, 1497–1504.
9 A. D. Taylor, J. Ladd, Q. Yu, S. Chen, J. Homola and S. Jiang, *Biosens. Bioelectron.*, 2006, **22**, 752–758.
10 C. Wei, M. Li and X. Zhao, *Front. Microbiol.*, 2018, **9**, 1–9.
11 X. Ma, X. Xu, Y. Xia and Z. Wang, *Food Control*, 2018, **84**, 232–237.
12 Q. Yu, T. Wu, B. Tian, J. Li, Y. Liu, Z. Wu, X. Jin, C. Wang, C. Wang and B. Gu, *Anal. Chim. Acta*, 2023, **1286**, 341931.
13 J. Dong, H. Zhao, M. Xu, Q. Maa and S. Ai, *Food Chem.*, 2013, **141**, 1980–1986.
14 L. Wang, X. Huo, W. Qi, Z. Xia, Y. Li and J. Lin, *Talanta*, 2020, **211**, 120715.
15 P. Wang, B. Luo, K. Liu, C. Wang, H. Dong, X. Wang, P. Hou and A. Li, *RSC Adv.*, 2022, **12**, 27940–27947.
16 S. Muniandy, S. J. Teh, J. N. Appaturi, K. L. Thong, C. W. Lai, F. Ibrahim and B. F. Leo, *Bioelectrochemistry*, 2019, **127**, 136–144.
17 Y. Ye, W. Yan, Y. Liu, S. He, X. Cao, X. Xu, H. Zheng and S. Gunasekaran, *Anal. Chim. Acta*, 2019, **1074**, 80–88.
18 S. Muniandy, K. L. Thong, J. N. Appaturi, C. W. Lai and B. F. Leo, *Sens. Diagn.*, 2022, **1**, 1209–1217.
19 M. Weston, A. H. Pham, J. Tubman, Y. Gao, A. D. Tjandra and R. Chandrawati, *Mater. Adv.*, 2022, **3**, 4088–4102.
20 T. N. Nguyen, V. D. Phung and V. Van Tran, *Biosensors*, 2023, **13**, 586.
21 J. Chen, C. Wang, X. Qin, X. Yang, C. Yang, H. Nie, H. Chen and H. Li, *Coord. Chem. Rev.*, 2023, **497**, 215433.
22 J. T. Wen, J. M. Roper and H. Tsutsui, *Ind. Eng. Chem. Res.*, 2018, **57**, 9037–9053.

23 R. W. Carpick, D. Y. Sasaki, M. S. Marcus, M. A. Eriksson and A. R. Burns, *J. Phys.: Condens. Matter*, 2004, **16**, 679–697.
24 D. C. Lee, S. K. Sahoo, A. L. Cholli and D. J. Sandman, *Macromolecules*, 2002, **35**, 4347–4355.
25 D. E. Wang, L. Zhao, M. Sen Yuan, S. W. Chen, T. Li and J. Wang, *ACS Appl. Mater. Interfaces*, 2016, **8**, 28231–28240.
26 D. J. Ahn, E. H. Chae, G. S. Lee, H. Y. Shim, T. E. Chang, K. D. Ahn and J. M. Kim, *J. Am. Chem. Soc.*, 2003, **125**, 8976–8977.
27 J. Yoon, S. K. Chae and J. M. Kim, *J. Am. Chem. Soc.*, 2007, **129**, 3038–3039.
28 H. Shen, J. Wang, H. Liu, Z. Li, F. Jiang, F. B. Wang and Q. Yuan, *ACS Appl. Mater. Interfaces*, 2016, **8**, 19371–19378.
29 S. Hussain, R. Deb, S. Suklabaidya, D. Bhattacharjee and S. Arshad Hussain, *Mater. Today: Proc.*, 2022, **65**, 2765–2772.
30 S. Ni, Z. Zhuo, Y. Pan, Y. Yu, F. Li, J. Liu, L. Wang, X. Wu, D. Li, Y. Wan, L. Zhang, Z. Yang, B. T. Zhang, A. Lu and G. Zhang, *ACS Appl. Mater. Interfaces*, 2021, **13**, 9500–9519.
31 H. R. Jia, Z. Zhang, X. Fang, M. Jiang, M. Chen, S. Chen, K. Gu, Z. Luo, F. G. Wu and W. Tan, *Mater. Today Nano*, 2022, **18**, 100188.
32 J. Chen, C. Yang, H. Nie and H. Li, *Spectrochim. Acta, Part A*, 2023, **293**, 122451.
33 A. D. Tjandra, M. Weston, J. Tang, R. P. Kuchel and R. Chandrawati, *Colloids Surf., A*, 2021, **619**, 126497.
34 Y. Jiao, Z. Zhang, K. Wang, H. Zhang and J. Gao, *Food Chem.: X*, 2023, **19**, 100798.
35 Y. K. Jung, T. W. Kim, J. Kim, J. M. Kim and H. G. Park, *Adv. Funct. Mater.*, 2008, **18**, 701–708.
36 S. Lee, J. Y. Kim, X. Chen and J. Yoon, *Chem. Commun.*, 2016, **52**, 9178–9196.
37 X. Sun, T. Chen, S. Huang, L. Li and H. Peng, *Chem. Soc. Rev.*, 2010, **39**, 4244–4257.
38 J. Lee, H. J. Kim and J. Kim, *J. Am. Chem. Soc.*, 2008, **130**, 5010–5011.
39 N. Duan, S. Wu, X. Chen, Y. Huang, Y. Xia, X. Ma and Z. Wang, *J. Agric. Food Chem.*, 2013, **61**, 3229–3234.
40 C. Sester, J. A. J. McCone, A. Sen, J. Vorster, J. E. Harvey and J. M. Hodgkiss, *Biophys. J.*, 2022, **121**, 2193–2205.
41 R. Joshi, H. Janagama, H. P. Dwivedi, T. M. A. Senthil Kumar, L. A. Jaykus, J. Schefers and S. Sreevatsan, *Mol. Cell. Probes*, 2009, **23**, 20–28.
42 Y. Fu, J. Wei, S. Yao, L. Zhang, M. Zhang, X. Zhuang, C. Zhao, J. Li and B. Pang, *Microchim. Acta*, 2022, **189**, 218.
43 S. Du, Z. Lu, L. Gao, Y. Ge, X. Xu and H. Zhang, *Microchim. Acta*, 2020, **187**, 627.
44 L. Zheng, G. Cai, W. Qi, S. Wang, M. Wang and J. Lin, *ACS Sens.*, 2020, **5**, 65–72.
45 R. Luo, Y. Li, X. Lin, F. Dong, W. Zhang, L. Yan, W. Cheng, H. Ju and S. Ding, *Sens. Actuators, B*, 2014, **198**, 87–93.
46 T. V. De Oliveira, N. D. F. F. Soares, N. J. De Andrade, D. J. Silva, E. A. A. Medeiros and A. T. Badaró, *Food Chem.*, 2015, **172**, 428–432.